

MIT Open Access Articles

*Moving beyond 99.9% Coulombic efficiency
for lithium anodes in liquid electrolytes*

The MIT Faculty has made this article openly available. *Please share*
how this access benefits you. Your story matters.

Citation: Hobold, Gustavo M, Lopez, Jeffrey, Guo, Rui, Minafra, Nicolò, Banerjee, Abhik et al. 2021. "Moving beyond 99.9% Coulombic efficiency for lithium anodes in liquid electrolytes." Nature Energy, 6 (10).

As Published: 10.1038/S41560-021-00910-W

Publisher: Springer Science and Business Media LLC

Persistent URL: <https://hdl.handle.net/1721.1/143495>

Version: Author's final manuscript: final author's manuscript post peer review, without publisher's formatting or copy editing

Terms of use: Creative Commons Attribution-Noncommercial-Share Alike



Moving beyond 99.9% Coulombic efficiency for lithium anodes in liquid electrolytes

Gustavo M. Hobold¹, Jeffrey Lopez^{2,6}, Rui Guo^{1,6}, Nicolo Minafra², Abhik Banerjee^{3,4}, Y. Shirley Meng^{3,*}, Yang Shao-Horn^{1,2,5,*}, Betar M. Gallant^{1,*}

¹Department of Mechanical Engineering, Massachusetts Institute of Technology, Cambridge, MA 02139

²Research Laboratory of Electronics, Massachusetts Institute of Technology, Cambridge, MA 02139

³Department of NanoEngineering, University of California San Diego, La Jolla, CA 92093

⁴Research Institute for Sustainable Energy (RISE), TCG Centres for Research and Education in Science and Technology (TCG CREST), Sector V, Salt Lake, Kolkata 700091, India

⁵Department of Materials Science and Engineering, Massachusetts Institute of Technology, Cambridge, MA 02139

⁶These authors contributed equally

*Corresponding authors: shmeng@ucsd.edu; shaohorn@mit.edu; bgallant@mit.edu

Abstract

As Li-ion battery cost decreases, energy density and thus driving range remains a roadblock for mass-market vehicle electrification. While Li metal anodes help achieve DOE targets of 500 Wh/kg (750 Wh/L), Li Coulombic efficiencies (CE) fall below 99.95+% required for 1000+ cycles. They are, however, closer than ever, having increased from <80% to 99.9% in the past five decades. Considering the remaining gap, we examine: 1) Historical strategies underlying increased CE; 2) Important interplays between electrolyte, solid electrolyte interphase (SEI) composition, plating/stripping kinetics, and Li morphology, which collectively determine performance; 3) The need for more data to robustly assess CE. While multiple electrolytes reach 98-99% CE over subsets of cycles, achieving >99% CE consistently throughout cycling is an as-yet unmet challenge. We highlight parameters only recently being experimentally measured at the Li interface and forward-looking strategies, representing new opportunities to refine understanding and rationally improve Li cycling in coming years.

Introduction

Following decades of development, lithium (Li) still cannot be used in metallic form as an anode in commercial rechargeable batteries. Theoretically, Li battery energy densities ($\sim 2,000$ Wh/L, with a capacity-paired metal oxide cathode¹) satisfy targets for future electric vehicles (EV, > 750 Wh/L).² However, steep requirements for reversibility, mandating Coulombic efficiency (CE) above 99.95% and likely above 99.99% for 80-90% capacity retention over 1,000 cycles, represent a performance goalpost that has not yet been reached. CE is defined as the ratio of the amount of Li that can be electrochemically stripped from the negative electrode compared to what had been plated on a preceding step. To serve as an accurate metric of Li anode reversibility, CE must be measured on a working electrode with no excess Li and with a counter electrode that contains a Li reservoir (*e.g.*, Cu||Li half cells).³ In liquid electrolytes, the limitation in Li reversibility and thus in CE arises from thermodynamic instability of all practically-relevant electrolytes at the Li potential (0 V *vs.* Li/Li⁺ = -3.04 V *vs.* SHE) due to the higher Fermi level of Li versus the lowest unoccupied molecular orbital (LUMO) levels of electrolytes,⁴ leading to formation of a surface layer on Li. Ideally, this layer, referred to as the solid electrolyte interphase (SEI),^{5,6} should be stable, electronically insulating, Li⁺-conducting, and chemically blocking to prevent sustained contact of the electrolyte and electrode,⁷ such as that formed between graphite and ethylene carbonate-based electrolytes in Li-ion batteries.⁸ However, unlike on graphite, existing electrolytes cannot form a fully-protective SEI on Li, resulting in parasitic consumption of solvents, of Li⁺ in the electrolyte and of active metallic Li⁰.

To date, no electrolyte has been able to support Li CE exceeding 99.9% over $>1,000$ cycles. An historical recounting of record-breaking CE reported for Li shows that liquid electrolyte development, which has been central to progressing towards a stable Li anode, has evolved through several stages (**Figure 1**). At a high level, two principles have guided electrolyte design: (1) Suppression of problematic solvent reduction on Li (*e.g.*, use of ethers as opposed to carbonates); (2) Selective *promotion* of certain reactions involving solvent and/or salt towards specific SEI phases (*e.g.*, LiF, polymers) thought to benefit Li reversibility. Together, these two principles aim to harness increasingly meticulous control over complex molecular trajectories (Li⁺, salt anions, solvent and additives) at the Li interface, and have achieved measurable success: many promising systems have come closer than ever to ambitious goals for CE, even breaching 99.9% over a portion of cycling in recent years. In this context, it is timely to ask whether there is a physical

basis to believe the remaining gap can be closed using liquid electrolytes. In this perspective, we highlight several promising phenomenological strategies that may yet, if perfected, deliver the needed advancements in Li anode performance, particularly if utilized together. However, we also argue that precise quantification of chemistry, electron/ion-transfer kinetics, and SEI morphology is still needed before a predictive theory of Li cycling can be created, which can crucially help steer rational strategies to improve CE.

Electrolyte trends and strategies leading to high CE

We begin with a necessary examination of the current benchmarks in Li CE and the pathway leading here. **Figure 1** plots incremental record CE values and the year in which each was reported; in a given year, a high-performing yet non-record-breaking value is omitted except in select cases where CE equals or exceeds 99%. As early-stage Li research focused largely on carbonate-based electrolytes, a reference point is set by 1 M LiClO₄ in propylene carbonate (PC),⁹ which achieved a CE of ~80% by 1974.¹⁰ (We herein report the number of decimal places used by the original authors wherever available, which varies study-to-study; see the **Source Data** file for more information). While modest improvement (CE = 83.6%, 1977) was subsequently achievable using additives,¹¹ carbonate solvents are particularly unstable at Li potentials due to their strongly-polar carbon-oxygen bonds and inability to form a protective SEI.¹² Thus, replacing carbonates with weakly-polar, more cathodically-stable ethers led to more substantial increases in CE.¹³⁻²⁰ This era also saw growing use of LiAsF₆ due to its improved safety over LiClO₄ and ability to passivate Al current collectors at cathode potentials.⁶ For example, 1 M LiAsF₆ in THF achieved a CE of 89.4% (1978),¹³ motivating use of more-stable 2-methyl-tetrahydrofuran (with 1-1.5 M LiAsF₆ salt), which reached a CE of 97.4% in the following year.^{15,17} Later, ether-based blends were introduced, such as LiAsF₆ in diethyl ether (DEE)/THF (CE = 97.6%, 1982)¹⁶ or ether/carbonate co-solvents having ethers as the primary constituent (*e.g.*, 1 M LiAsF₆ in 12% PC or 30-35% EC in DOL, CE = ~98%, 1992).²⁰ Following these gains, remarkably, subsequent CE improvements appear to have largely stagnated for over two decades while greater strides were being achieved with Li-ion batteries, which were undergoing commercialization throughout the 1990s; Li-ion batteries employ a graphite anode with an SEI that is sufficiently stable in carbonate electrolytes.

Following renewed interest in Li since the 2010s, the field has witnessed the emergence of powerful new electrolyte design strategies. **Figure 1** makes clear that CE gains breaching 99%

have been overwhelmingly favored by use of electrolyte fluorination²¹ which now includes newer salts (beyond LiPF₆/LiAsF₆), specifically lithium bis(fluorosulfonyl)imide (LiFSI) and lithium bis(trifluoromethanesulfonyl)imide (LiTFSI), and fluorinated solvents such as fluoroethylene carbonate (FEC).²² While these salts started to see application in the late 1990s,⁶ they became leading contenders for use with Li in the 2010s when incorporated as part of more-complex electrolyte strategies. For example, by using 0.5 M/0.5 M LiFSI/LiTFSI in DOL:1,3-dimethoxyethane (DME), Miao *et al.*²³ developed the concept of a dual-salt electrolyte, finding a CE of 99% (2014), higher than that of an analogous 1 M LiTFSI DOL/DME (80.1%).²³ Additionally, using these salts individually but at higher concentrations (~4-11 M in ethers and carbonates)—possible due to their uniquely high solubilities compared to more conventional salts⁶—led to further gains, *e.g.* a CE of 99.1% was reported in 2015 using 4 M LiFSI in DME.²⁴ At high concentrations (>> 1 M, also described as ‘superconcentrated’ or ‘solvent-in-salt’ at concentrations where all solvent become coordinated to Li⁺),²⁵ both LiTFSI and LiFSI exhibit significant degrees of Li⁺-anion contact-ion pairing (CIP),²⁶⁻²⁸ which places the anion within the coordination environment of Li⁺ and lowers the anion’s LUMO with respect to both bulk and coordinated solvent molecules.²⁹ This increases the driving force for an anion to participate in beneficial SEI-building reactions while Li⁺ is being plated, as will be discussed later. Aside from fluorinated salts, fluoroethylene carbonate (FEC) solvent has also been an electrolyte constituent of growing importance. As demonstrated by Li *et al.*, the combination of FEC with a yet-higher concentration (7 M) of LiFSI can achieve 99.6% CE.³⁰ (We note that electrolyte concentrations are stated as reported by the original source, *i.e.*, typically as molarity (mols of salt per liter of solution); however, the reader should bear in mind that this approximation can fail, particularly in high-concentration electrolytes where salt volume can be significant. In these instances, molality (mols of salt per mass of solvent) is a preferred metric, though seldom reported by original sources.)

Similarly-high CEs have been reported subsequently using electrolyte engineering strategies, which we define to include use of multi-component electrolyte formulations and nontraditional solvents. For instance, 1 M LiTFSI/2 M LiFSI/3% LiNO₃ in DOL/DME reached a CE of 99.6% in 2019.³¹ In addition, it has more-recently been possible to achieve the beneficial aspects of superconcentrated electrolytes with LiFSI and/or LiTFSI at lower salt concentrations in so-called “localized high-concentration electrolytes” (LHCE) electrolytes.^{29,32,33} These systems

retain local Li⁺-anion paired domains found in highly-concentrated electrolytes using, *e.g.*, DMC solvent, yet diluted within more weakly-coordinating fluoroethers such as bis(2,2,2-trifluoroethyl) ether (BTFE), lowering the total salt concentration (≤ 2.5 M)^{32,33} and achieving a CE of up to 99.5%.³³ Because LiTFSI and LiFSI are readily solvated, they can even be utilized with fully non-polar solvents such as pressurized liquefied gas electrolytes³⁴⁻³⁶ (*e.g.*, CH₃F), recently breaching 99.9% CE even at low salt concentrations (0.3 M LiTFSI in CO₂/CH₃F + 0.3 M THF).³⁵ This system is, to the best of our knowledge, the highest Li CE reported to date, given as the average CE of cycles 100-400 in a Cu||Li cell.

In addition to record-setting systems, the reported CE of a larger number of representative electrolyte formulations, including additives, are organized in **Figure 2a** as a function of salt and in **Figure 2b** as a function of fluorine molarity of the electrolyte. Among the former, the use of LiNO₃ as an additive is a recurring motif in many high-CE systems, including several that are record-breaking, and can be readily combined with other electrolyte strategies to boost CE. Where fluorination is concerned, it is apparent that there is no simplistic monotonic trend of CE with generic fluorine content across a wide range of electrolytes; certain salts (such as LiPF₆) indeed exhibit large amounts of scatter in contrast to others (LiFSI). Thus, while increasing the F concentration of ‘beneficial’ fluorination is one seemingly-reliable strategy to reach high CE, the chemistry and decomposition kinetics of the F-source represent an area where more understanding is needed. In this context, it is interesting to note that LiPF₆ recently resurged with the use of a blend of fluorinated solvents (1 M LiPF₆ in FEC/3,3,3-fluoroethylmethyl carbonate (FEMC)/1,1,2,2-tetrafluoroethyl-2',2',2'-trifluoroethyl ether (HFE)), yielding a CE of 99.2%,³⁷ the only LiPF₆-based electrolyte to surpass 99% to the best of our knowledge. Overall, the data in **Figure 1-2** show that there are already multiple successful routes to high (>99%) CE, indicating that there may not be a single “winner-takes-all” strategy to generate a reversible Li anode.

To begin to more-finely differentiate between high-performance electrolytes in coming years, it will be critical to understand precisely how capacity is lost from a microscopic viewpoint, processes which become increasingly challenging to probe when exceeding 99% CE. As we discuss next, the groundwork for this understanding is still being laid very recently with the emergence of quantitative techniques to learn more about the elusive fate of Li inventory in the battery.

Connecting Li morphological trends with CE

To interpret macroscopic values of CE, it is first essential to understand the microscopic origin of how Li is lost during a plating/stripping cycle, *i.e.* the mechanism by which Li becomes electrochemically inactive. Two modes of Li deactivation predominate: (1) Loss to form the SEI directly, resulting in ionic Li^+ entrapment; and (2) Encapsulation of electronically-disconnected Li^0 . While these processes have long been qualitatively discussed,^{5,38} their relative inventories were not quantitatively known. Recently, Meng *et al.* provided key insights using titration gas chromatography (TGC), an analytical technique that quantifies H_2 evolved upon Li^0 hydrolysis by reacting cycled SEI with water³⁹ ($2 \text{Li} + \text{H}_2\text{O} \rightarrow 2 \text{LiOH} + \text{H}_2$). The relative capacities lost from encapsulated Li^0 vs. Li^+ in the SEI are strongly dependent on electrolyte composition (**Figure 3a**): encapsulated Li^0 dominates active Li loss for electrolytes with CE <95%, such as those found in 1 M LiPF_6 in EC/EMC.³⁹ Moving from a LiPF_6 /carbonate-based to a liquefied-gas electrolyte (0.3 M LiTFSI in THF/ CO_2 / CH_3F) yields a substantial increase in CE (from 82% to 91.5% in the first cycle). This difference can be explained by a substantial decrease in encapsulated Li^0 ,³⁹ resulting in a larger proportional contribution of SEI Li^+ to the overall capacity loss at high CE. Hence, Li capacity loss occurs in two distinct regimes: 1) At SEI Li^+ /unreacted $\text{Li}^0 < 1$, encapsulated Li^0 is responsible for proportionally more, and in some cases nearly all of the capacity loss, which generally corresponds to low-to-moderate CE; and 2) At SEI Li^+ /unreacted $\text{Li}^0 > 1$, capacity loss is primarily due to SEI Li^+ , and corresponds to high CE values. The transition between regimes involves some scatter but occurs at a CE of ~90-95% in **Figure 3b**.

In the Li^0 -dominated regime (lower CE), electronically-inactive Li^0 corresponds to higher deposition porosity (**Figure 3b**). Computationally-reconstructed images of the electrodes acquired by cryogenic transmission microscopy (Cryo-TEM) show large voids in deposited Li (filled teal regions up to ~1 μm in size, **Figure 3c**) totaling 17% porosity for the carbonate-based electrolyte. The high amounts of isolated Li^0 in conventional carbonate-based electrolytes can be attributed to the evolution of mossy and porous Li nanostructures, as has also been observed by Cryo-TEM.⁴⁰ These high-surface-area Li deposits exacerbate reactivity with electrolyte, leading to substantial cell impedance and overpotentials^{41,42}. Moreover, if the electrode is not sufficiently electronically-percolated during stripping, SEI will surround and neck Li, which becomes electronically-

inaccessible and hence electrochemically-inactive, ultimately contributing to capacity loss and low CE.³⁹ In these electrolytes, internal or stack pressure applied to the electrodes has recently been demonstrated to substantially reduce porosity of electrochemically-deposited Li and increase CE^{43,44}.

An instructive example of how electrolytes change from Li⁰-dominated to SEI-dominated is found through use of a beneficial additive in an otherwise Li⁰-dominated electrolyte. Compared to a non-fluorinated solvent 1 M LiPF₆ EC/EMC, which lies in a Li⁰-dominated regime with an Li⁺/Li⁰ ratio of 0.28, FEC additive in this same electrolyte (1 M LiPF₆ EC/EMC + 10% FEC) increases CE by reducing capacity loss to encapsulated Li⁰ (**Figure 3a**), increasing the Li⁺/Li⁰ ratio to 5.2 and putting it in the SEI-dominated regime.³⁹ Supporting these findings, addition of FEC has been shown independently *via in situ* nuclear magnetic resonance (NMR) to promote more Li loss to SEI than a base carbonate electrolyte (1 M LiPF₆ EC/DMC), leading to thicker SEIs.⁴⁵

Electrode morphology is also affected by the transition from a Li⁰-dominated to an SEI-dominated regime. Porosity, in particular, depends on the electrolyte chemistry and reduces significantly from 17% in 1 M LiPF₆ EC/EMC (Li⁺/Li⁰ = 0.28) to 2% in 2 M LiTFSI/4 M LiFSI DME (**Figure 3b**), which has a higher SEI contribution to capacity loss at Li⁺/Li⁰ = 0.64 (**Figure 3a**). Moving to an electrolyte in the SEI-dominated regime, 0.3 M LiTFSI THF/CO₂/CH₃F (Li⁺/Li⁰ = 2.4, 1st cycle CE = 91%), further reduces electrode porosity to 0.9%, corresponding to densely-packed Li deposits (**Figures 3e**).⁴⁰ As the deposited Li is better electronically-percolated, Li can be oxidized uniformly during stripping, rendering the high CE values observed in the SEI-dominated regime³⁹ and resulting in a capacity loss that is almost entirely due to SEI formation. Overall, these results are highly consistent with studies that routinely find rougher, more porous Li deposits in lower-CE electrolytes and smoother, less porous deposits in higher-CE electrolytes.^{26,30,31} Given that high-CE electrolyte strategies shift electrolytes towards SEI-dominated CEs,⁴⁶ the SEI's electron/Li⁺-transfer kinetics and Li⁺ transport will become key differentiators at high CE.

Towards establishing descriptors governing CE

Here we discuss and propose possible descriptors that correlate CE, associated Li morphologies, and electrolyte composition. In classical metal electrodeposition theory, morphological features of metal deposits are correlated with reaction kinetics and ion transport/diffusivity.⁴⁷ High ion

diffusivity (D) combined with low reaction rates ($k \sim \frac{j}{Fc}$, where j is current density, F is the Faraday constant and c is cation concentration) leads to a rate-controlled reaction and uniform plating.⁴⁷ Low D and fast reaction rates result in diffusion-limited plating and the formation of roughened surfaces and dendrites,⁴⁸ where diffusion is too slow to supply ions needed by interfacial reactions.⁴⁷ Unfortunately, understanding and controlling reversible Li electrodeposition in aprotic electrolytes is complicated by the presence of the SEI,⁴⁹ which can have transport properties such as Li^+ transference number and diffusivity distinct from bulk electrolytes, along with interfacial kinetics of Li plating/stripping substantially different from that of the innate Li/electrolyte interface.⁵⁰ In this context, previous experimental observations have shown that decreasing current density facilitates growth of increasingly smooth Li in Li/PEO⁵¹ and Li/carbonate⁵² systems. This effect has also been examined by computational studies,⁵³ which reveal that diffusion-limited conditions at the interface (*e.g.* reaching zero Li^+ concentration at Sand's time⁵⁴) combined with a chemically-heterogeneous SEI⁵³ (giving rise to nonuniform current densities) facilitates formation of Li dendrites. More recently, the coupling between interfacial kinetics and transport on Li plating morphologies is shown elegantly by coarse-grained molecular dynamics (MD) simulations of Li plating, revealing that slower reaction rates and/or faster diffusion in hypothetical SEI promote smoother, denser Li deposits.⁵⁵ Analytical expressions derived using linear stability analysis agree with these results from MD, and further suggest that, in polymers (of which the SEI may be constituted), high stiffness⁵⁶ and surface energy can facilitate smooth Li plating.⁵⁷ On the other hand, increasing the current densities demanded during stripping can facilitate dissolution/smoothing of previously-formed mossy or roughened Li, leading to a smoother Li/electrolyte interface.^{58,59} This beneficial effect originates from high current densities and preferential stripping at local inhomogeneities of Li deposits due to stronger concentration gradients, helping to restore a more planar morphology.⁵⁸ Thus, while slow plating is desired for smooth Li deposition, fast stripping may be desirable for high CE. This phenomenon suggests that asymmetric cycling could aide performance and highlights the existence of important effects beyond electrolyte chemistry that may affect CE.

These learnings have catalyzed effective strategies⁵⁷ to suppress Li dendrites such as introduction of three-dimensional current collectors⁶⁰⁻⁶² (to lower local current densities and eliminate mechanical expansion of the anode), control of cell stack pressure,^{63,64} and creation of

artificial SEI⁶⁵⁻⁶⁷ (to potentially alter ion transport, surface reactivity and surface energy), and subsequently enhance CE. However, it is difficult to directly apply them to understand possible physical origins underpinning the significant advance in CE associated with different liquid electrolytes (**Figure 1**) and envision strategies of electrolyte design to further increase CE, which can be attributed to the lack of systematic experimental data and understanding of electrolyte-dependent SEI properties. To illustrate this, **Figure 4a** shows reported CE of different electrolytes as a function of $\frac{j}{FCD}$, where D is the apparent concentration-dependent Li⁺ diffusivity in the bulk electrolyte estimated from separate studies given that D in the SEI is largely not accessible at present (see **Source Data** for supporting values). The key hypothesis in this analysis is that uniform and smoother Li plating and stripping, and thus higher CE, will result from decreasing current densities normalized to Li⁺ transport as previously discussed. Unfortunately, no trend can be discerned in **Figure 4a**, and we hypothesize that the large scatter can be attributed to several factors: 1) Exchange current densities for Li plating/stripping, which are not captured by the parameter $\frac{j}{FCD}$, can be strongly electrolyte-dependent⁵⁰ and hence may greatly influence the coupling of kinetics and transport at the interface; 2) Li⁺ diffusivity in the SEI can be greatly different from that in bulk electrolyte. For example, Guo *et al.* have found the diffusivity of phase-pure, nanocrystalline LiF or Li₂O thin films on Li to be several orders of magnitude higher, at 1.8×10^{-9} cm²/s (Li₂O) and $\sim 4.5 \times 10^{-10}$ cm²/s (LiF), than their bulk crystalline powder counterparts of $\sim 10^{-12}$ cm²/s,⁶⁸⁻⁷⁰ but significantly lower than that of liquid electrolytes (10^{-5} to 10^{-8} cm²/s).⁶

While Li⁺ diffusivity in the native SEI remains scarcely reported in the literature, electrolyte-dependent exchange current densities of Li plating/stripping at the Li/electrolyte interface have started to become available in the past five years, allowing us to examine the role of current density (j) normalized to the exchange current density (j_0) on CE for the first time. Li⁺ exchange current density is challenging to precisely measure given that the real surface area changes as Li is plated/stripped from the electrode. As such, we next describe a few select well-controlled studies that systematically investigate j_0 in various electrolytes, noting that exchange current on Li should be interpreted as an estimated value with some error rather than an accurate measure of true areal charge-transfer kinetics given the challenges mentioned above.

Systematic cyclic voltammetry experiments^{50,71,72} reveal that j_0 varies greatly across different electrolytes and measurement conditions (**Figure 4b**). Contact-ion pairing has been shown

to reduce j_0 ;⁵⁰ this is also represented in **Figure 4b** where, at least for particular electrolyte compositions, j_0 decreases with increasing salt concentration (LiTFSI from 0.52 to 2.75 M in tetraethylene glycol dimethyl ether (TEGDME, G4), red data).⁷² Additionally, j_0 decreases as the SEI forms. Indeed, j_0 measured with ultramicroelectrodes at fast scan rates (>10 V/s) can be orders of magnitude higher than those of similar electrolytes measured at low rates^{71,72} (1 mV/s) in **Figure 4b**, for example, comparing 1 M LiPF₆ in EC/DEC/FEC at >10 V/s⁵⁰ and 1.1 M LiPF₆ in ethyl methyl carbonate (EMC)/FEC at 1 mV/s,⁷¹ which vary by over two orders of magnitude with the latter allowing more time for the SEI to develop. Therefore, exchange current densities measured at high scan rates⁵⁰ are not directly relevant to CE, given that CE is typically measured with long exposure of Li to electrolytes and low current densities (*e.g.* <1 mA/cm²_{Li}), lower than the exchange current densities at high scan rates (**Figure 4b**).

Here we correlate CE with exchange current densities from two studies that report both parameters under comparable conditions^{71,72}, where the exchange current density reflects that of SEI-covered Li (j_0^{SEI}). At fixed j used in CE measurements, decreasing j_0^{SEI} (red data in **Figure 4c**) to values lower than j is correlated with increasing CE, which can be attributed to more homogeneous local current densities associated with smoother Li plating and stripping.⁷² This argument is in agreement with previous observations that proposed decreased j_0 to *increase* CE by forming a passivating SEI,⁷² promoting larger, denser deposits⁷³ as observed in ether-based electrolytes with LiNO₃.⁷⁴ To capture previous computational learnings that slower reaction rates and/or faster diffusion can promote smoother, denser Li deposits,⁵⁵ and to reflect the interplay between kinetics and diffusion, we correlate CE as a function of j_0^{SEI}/FcD in **Figure 4d**, where electrolyte diffusivity (D) in bulk is used here due to lack of information of Li⁺ diffusivity in the SEI. When j_0^{SEI}/FcD is greater than 1, increasing j_0^{SEI} with respect to FcD (red data in **Figure 4d**) reduces CE, which can be attributed to the formation of less smooth Li deposits.⁷² On the other hand, having j_0^{SEI} much lower than j (~ 10 times lower, *i.e.*, $j/j_0^{\text{SEI}} > 10$ in FEC-containing electrolytes) is correlated with reduction in CE, which is associated with having $j_0^{\text{SEI}}/FcD < 1$ (blue data in **Figure 4c,d**). Under this scenario, large overpotentials needed to sustain a given applied current (due to small j_0^{SEI}) promote formation of small Li nuclei and more nonuniform local current densities for Li plating/stripping. We note that CE in some electrolytes (*e.g.* 1 M LiPF₆ in FEC/ethyl acetate (EA), yellow data in **Figures 4c,d**) have weaker dependence on j/j_0^{SEI} and

j_0^{SEI}/FcD than others, indicating the need for further systematic studies on a much broader number of electrolytes.

Whether these observations generalize to practical conditions in which SEI mediates Li-electrolyte exchange remains to be explored. These correlations raise many questions and highlight the critical need to better understand SEI chemistry, morphology and coupled kinetic and transport properties, which are ultimately electrolyte derived. Below we discuss limited information on electrolyte-dependent SEI compositions and highlight research opportunities towards controlling SEI *via* electrolyte design.

Towards revealing and controlling deposited Li and its interface for high CE

Progress beyond 99.9% CE requires understanding and mastering of how electrolytes become reduced on the Li surface to form the SEI. Peled³⁸ proposed a mosaic structure of the interface based on understanding developed in carbonate electrolytes, consisting of multiple inorganic and organic species formed from electrolyte decomposition; near the Li surface are compact layers of inorganic species like Li₂O and LiF, which are most-reduced and thus thermodynamically stable. Nearer to the electrolyte, the layers consist mainly of oligomer species (polyolefins) and semicarbonates. Recent advances in the CE of Li/electrolyte systems shed new insights into possible SEI compositions, properties and formation mechanisms giving rise to higher CE than those in carbonates. LiF, in particular, has received substantial focus because it has been found in the SEI of most high-CE electrolytes given the overwhelming reliance on fluorinated salts and solvents. The beneficial role of LiF in the SEI on CE has been attributed to its presumed electronically-blocking nature,²¹ high chemical stability,⁷⁵ and proposed ability to support uniform Li⁺ flux in the SEI.⁷⁶ For example, high CE of electrolytes based on fluorosulfonylimide salts (LiFSI/LiTFSI) has been attributed to an SEI that is rich in LiF,^{31,37} and more chemically-homogeneous than those formed in carbonates with hexafluorophosphate salts.⁷⁷ While increasing fluorination in both solvents and salts appears to correlate with increasing CE (**Figure 1**), the effectiveness of specific F-donor molecules can vary (**Figure 2b**). For example, superconcentrated ~5 M LiPF₆ or 8.5 M LiTFSI(only)-based electrolytes do not lead to exceptional CE values compared to their 1 M counterparts (from 82% in 1 M LiPF₆/DMC to 91% in 5 M LiPF₆/DMC, and ~30% in 8.5 M LiTFSI/DMC)²⁶ whereas 10 M LiFSI-based electrolytes have CE >99%.²⁶ LiFSI has a highly reactive fluorine bound to the S of sulfone (a leaving group),^{78,79} while LiTFSI

displays a trifluoromethyl substituent with less-reactive fluorine despite possessing the same sulfonylimide backbone. LiFSI is reported to render an SEI that is mostly Li_2O ³⁰ and LiF ^{23,26,30}, with reportedly no organofluorine.^{26,30} On the other hand, the fluoroalkyl substitution in LiTFSI can yield an organofluorine-rich interphase^{23,31} and low CE²³ unless paired with more beneficial co-salts such as LiFSI ^{23,31} or LiNO_3 .^{31,80} Similarly, fluoroalkylated molecules (*e.g.*, $\text{CF}_3\text{-EC}$) that leave behind organofluorine phases in the SEI have been reported to be detrimental to CE.⁸¹ Unfortunately it is not straightforward to create artificial SEIs to mimic successful electrolytes and achieve high CE. For example, recent work by He *et al.*⁷⁵ found that pre-formed, single-phase LiF on Li (with thickness of ~10-100 nm, representative of a native SEI), synthesized by metal-fluorinated gas reaction, is too resistive to avoid Li plating instabilities even at low currents. Given that LiF may be unavoidable with future electrolyte systems, optimizing its formation to yield dense but thin LiF interfaces limited to a few nanometers, and combined judiciously with polymeric phases, offers a compelling strategy to control and tune exchange current densities, Li diffusivity and mechanical properties needed to maintain smooth Li plating and stripping (**Figure 4d**) and high CE.

Cryo-TEM, a tool that has seen recent adoption due to its ability to resolve crystalline atomic lattices while preserving delicate chemical composition and spatial features, has been central to recent evolution in understanding of SEI morphology. Cryo-TEM has already revealed that interphases in some high-CE systems (1 M LiPF_6 EC/DEC + 10% FEC) consist of a thick amorphous matrix of presumed organic nature that coexist with nanoscopic (~5 nm) crystalline inorganic phases of Li_2O and Li_2CO_3 .^{82,83} In 1 M LiPF_6 EC/DEC, deposit regions of more compact morphology were observed to be richer in O- and C-containing species such as Li_2O and Li_2CO_3 compared to more porous structures, with no apparent difference in fluorine content.⁸⁴ Similar studies with the same electrolyte but added FEC also indicate that fluorine deposits might be too sparsely distributed to provide any function to the SEI.⁸⁵ As such, Cryo-TEM has been important in confirming and refining SEI models that have long been hypothesized (*e.g.* mosaic, layered structures) but for which there was limited direct evidence until recently. Given that relatively few electrolyte-derived SEI have been examined so far, Cryo-TEM is likely to remain a central tool in coming years as SEI models continue to be refined to become more precise and nuanced for different electrolytes.

The compositions and properties of organic SEI phases formed from solvent reduction or reactivity with Li are more challenging to discern than inorganic components and are elusive to even the most modern techniques like Cryo-TEM. Their role in shaping Li morphologies and CE represents an important frontier in the science and engineering of the SEI. In contrast to carbonates, high-CE-supporting solvents such as FEC are hypothesized to reduce towards cross-linked polycarbonates which are more chemically stable and provide elasticity to the SEI.⁸⁶ Similarly, DOL is known to polymerize in the presence of Lewis acids, incorporating polyethylene oxides in the SEI.²⁰ Whether these elastomers are beneficial for purely mechanical reasons (*i.e.*, they can buffer volume changes of Li during plating/stripping as has been suggested⁴⁹), or whether they also present intrinsically favorable electron-Li⁺ exchange kinetics and transport will be rich areas of further study. Hence, emerging tools that can report on the SEI with chemical precision and direct measurements of surface and transport properties are of interest. In this light, *operando* measurements of gas byproducts (e.g., C₂H₄, CH₄, CO, CO₂) generated during Li cycling have been recently shown capable of resolving specific solvent reduction mechanisms in carbonates and even differentiating their branching ratios quantitatively as a function of salt or applied current density,⁸⁷ information that is difficult or inefficient to obtain using more-conventional *ex situ* analysis methods. Other promising emerging experimental tools for direct surface analysis of organic SEI phases include *in situ* solid state nuclear magnetic resonance (NMR)⁴⁶ and *operando* infrared spectroscopy,⁸⁸ which are able to provide additional chemical resolution to disambiguate organic moieties. Collectively, coming years are poised to see increasingly-refined understanding of the SEI composition and its properties, which will inform design guidelines for new electrolyte solvents, salts, and additives that can achieve more-precise tailoring of interphase reactions at the Li interface.

Achieving a CE beyond 99.9% will very likely require cell design strategies beyond that of electrolyte and SEI design. Application of internal or cell stack pressure, which reduces electrode porosity, can substantially increase CE as exemplified in 1 M LiPF₆ EC/DEC electrolyte, which increased from 92.6% (30 psi) to 96.8% (600 psi). Unfortunately, similar gains were not seen in a high-CE electrolyte (1 M LiFSI in fluorinated 1,4-dimethoxybutane), in which the CE decreased from 99.4% to 99.1% over the same pressures,⁸⁹ highlighting that such strategies cannot overlook the importance of the electrolyte and SEI chemistry, which will remain crucial to perfect.

Whether these findings generalize to other high-CE electrolytes remains to be studied as the community seeks more examples of electrolytes beyond 99.9% CE.

Finally, it is important to note that concepts of CE must be interpreted cautiously as researchers increasingly design and test prototype full cells that combine Li metal anodes with intercalation cathodes, as CE in these cases will conflate Li and cathode losses. While intrinsic Li anode reversibility—as reflected in all Li CE metrics used in this paper—remains the fundamental and rigorous metric to compare Li cycling performance across different electrolyte formulations, CE of full Li cells will always provide the more-accurate information on cell capacity fade and cycle life and can highlight unexpected factors. For instance, a recent study showed that the per-cycle capacity retention of a Li-NMC battery can vary substantially depending on the thickness of the Li foil used. In a > 99% CE electrolyte (1.5 M LiFSI in DME/TTE), both anode-free and thick-Li (50-200 μm) configurations lead to an excessively-porous electrode, inviting Li-electrolyte reactions that lead to sudden cell death, whereas a thin (20 μm) pre-existing film leads to the formation of a more-stable Li-electrolyte interface that optimizes capacity retention.⁹⁰ Consequently, it is becoming clear that additional considerations beyond intrinsic Li plating/stripping CE can affect full-cell cycle life and represent an expanding area of future study. Ideally, future studies in prototype Li full cells should be conducted rapidly to evaluate emerging electrolyte systems showing promise in Cu||Li cells. Ideally, such measurements should be holistic and examine capacity retention data both using Li foils (with careful attention paid to thickness) and in so-called ‘anode-free’ configurations.

Outlook

While >99.9% CE has not yet been achieved over the entire life cycle of a >1,000-cycles Li-metal battery, 99.9% has been achieved in individual cycles, showing that this metric is not physically out of reach in liquid electrolytes. In the nearer term, judicious combinations of existing strategies, like optimized application of stack pressure to further minimize electrode porosity for high-CE electrolytes^{64,89} may help to increase the proportion of cycles that can exceed 99.9%. However, moving beyond 99.9% CE — where Li^+ lost to form the SEI is expected to overwhelmingly dominate remaining inefficiencies, at least at lower cycle numbers — will require further improvements in electrolytes.

Emerging chemistries may build strongly on successful precedence set by effective fluorinated chemistries like LiTFSI, LiFSI and FEC (among others) while addressing their shortfalls. For instance, imide-based salts have long been known as impractical for use in beyond-LiNi_xMn_yCo_{1-x-y}O₂ batteries due to their anodic instability at >4.5 V vs. Li⁺/Li.⁹¹ Similarly, FEC, a widely-used solvent in all-fluorine electrolytes, releases HF at moderate temperatures (> 40 °C), particularly in the presence of Lewis acids,⁹² which may pose challenges to its practical use as a base solvent. Fortunately, these challenges have started to be overcome by emerging molecularly-designed solvent chemistries (*e.g.*, fluoroethers⁹³, sulfonyl-fluorides^{78,79} and sulfones^{94,95}) engineered to suppress corrosion and provide stability at cathode potentials, thus enabling the use of imide-based salts like LiFSI and LiTFSI at high voltages. As such, these systems have proven to be excellent sandboxes, providing insight into how to gain control over the electrochemical reactions that occur at Li interfaces, with a large design space still to be explored for Li. We note that other emerging cathode chemistries (*e.g.*, Ni-rich,⁹⁶ gas-conversion,⁹⁷ sulfur⁹⁸) will also dictate further constraints to which a successful Li electrolyte must abide.

Given the role that additives have played over the years in boosting individual electrolytes at lower CE (**Figures 1 and 2**), the identification or design of new classes of additives that work concertedly with leading electrolytes such as HCE or LHCE systems will be a compelling path forward. Such considerations will require careful understanding of how existing additives work, and of the underlying principles that help predict how such additives function, whether as a beneficially reactive component of the Li⁺ coordination sphere or as a repair agent within the free solvent. Given that discovery of many leading additives has been phenomenological over the years, the ability to rationally design new functional electrolytes is an exciting prospect, noting that such efforts can also complement identification of new solvents and salts as described above. In this light, we believe the field is poised to benefit strongly from contributions of synthetic and computational chemistry in coming years.⁹⁹

Further improvements will benefit from improved understanding of the SEI, in particular, by developing quantitative understanding that can be encoded in useful descriptors that help to universalize the integrated effects of thermodynamics, kinetics and transport at the interface. Our assessment herein already suggests intriguing possibilities, such as the potential to tailor the ideal operating regime (current density) to the particular electrolyte/SEI combination and precisely balance kinetics and diffusion. The emergence of possible new cycling protocols, including

plating/stripping current density asymmetry to better control morphology evolution over time, will invite new opportunities to both sense and control Li battery systems in dynamic and complex conditions.

Finally, as performance gains continue, the need for well-established cycling protocols for Li metal is becoming a community-wide imperative to make fair comparisons among different systems and laboratories.^{3,100} High-precision coulometry will be unavoidable to enable resolution of inefficiencies of less than 0.01%.¹⁰¹ It is worth mentioning that when approaching such high CE, the role of minor electrolyte impurities can become substantial for Li-based systems, and may become an inadvertent differentiator across suppliers and laboratories if not exceedingly well-controlled. In the 1990s, commercialization of Li-ion batteries helped to address this factor and equipped researchers to best contribute to the technology development by ensuring supply of high-purity optimum electrolytes. The same is now needed for Li: industry support among chemical suppliers, battery manufacturers and research laboratories undoubtedly holds the highest chance of success of seeing rechargeable, long-lived Li metal batteries on the timescale demanded by our planet.

Acknowledgements

G.M.H., R.G., B.M.G. acknowledge support from the National Science Foundation under award number 1804247. J.L. acknowledges support by an appointment to the Intelligence Community Postdoctoral Research Fellowship Program at the Massachusetts Institute of Technology, administered by Oak Ridge Institute for Science and Education through an interagency agreement between the U.S. Department of Energy and the Office of the Director of National Intelligence. Y.S.-H. and N.M. acknowledge the financial support of the Assistant Secretary for Energy Efficiency and Renewable Energy, Vehicle Technologies Office, under the Advanced Battery Materials Research (BMR) Program, of the U.S. Department of Energy under Contract No. DE-AC02-06CH11357, Subcontract No. 9F-60231. A.B. and Y.S.M acknowledge the Zable Endowed Chair fund for energy technologies for efforts related to this work.

Competing Interests

The authors declare no competing interests.

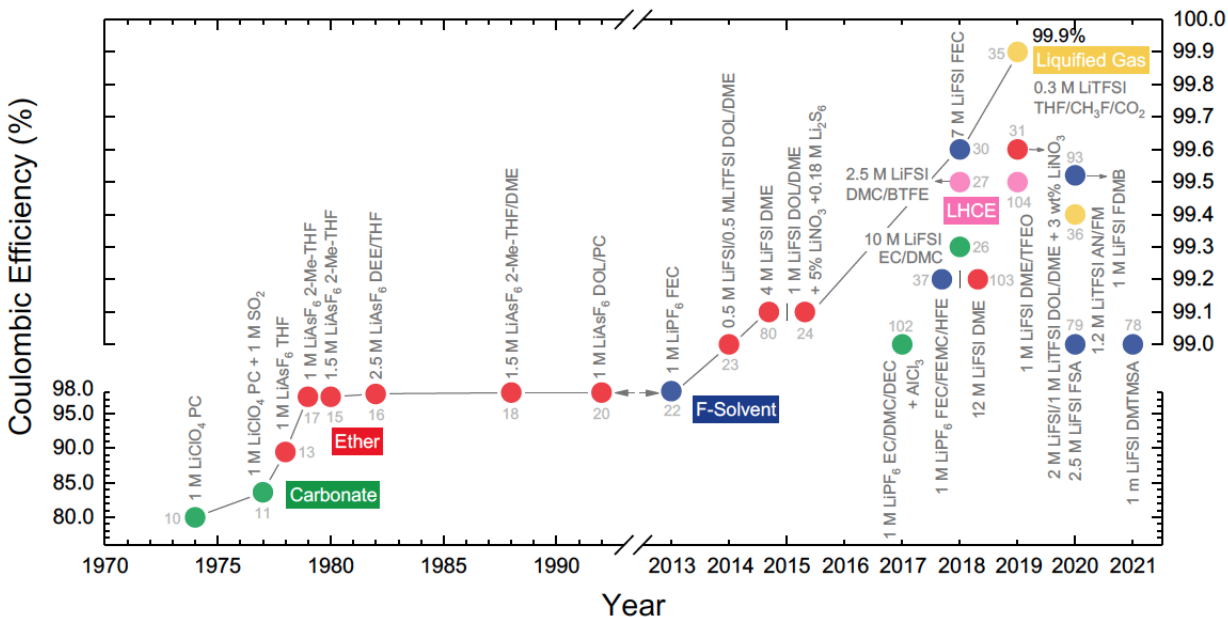


Figure 1 | Historical electrolyte strategies towards Li metal reversibility. (a) Benchmarking of published record-breaking Coulombic efficiency (CE) of Li plating/stripping in liquid electrolytes on “Li-free” working electrodes with a Li counter electrode. Based on availability of data, this figure highlights as-reported breakthrough CEs vs. their year of publication. CE data that obtained high numbers in a given year, but which did not break the cumulative record, are omitted, with the exception of select representative systems that exceeded 99%. Cycling protocols and additional details with references can be found in the **Source Data** file. CE data for electrolytes 1 M LiPF₆ EC/DMC/DEC + AlCl₃, 12 M LiFSI DME and 1 M LiFSI DME/tris(2,2,2-trifluoroethyl)orthoformate (TFEO) are collected here,¹⁰²⁻¹⁰⁴ with all others cited in the main text.

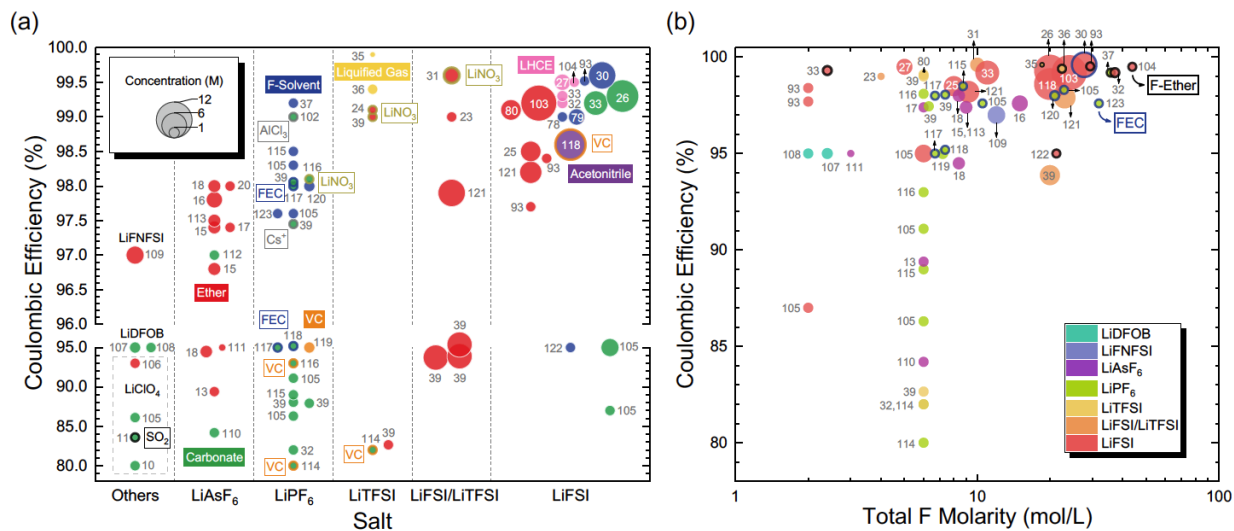


Figure 2 | Coulombic efficiency of select electrolyte systems. (a) Compendium of reported CE of published electrolytes categorized by salt species (horizontal axis), solvent (marker fill color), additive (marker border color), and salt concentration (marker size). (b) CE as a function of total atomic fluorine content in both the salt and solvent, estimated using salt concentration and solvent density. Cycling protocols and additional details (current collector, current density, cell construction) for a-b can be found in the **Source Data** file. References not cited elsewhere in the text are collected here.¹⁰⁵⁻¹²⁴

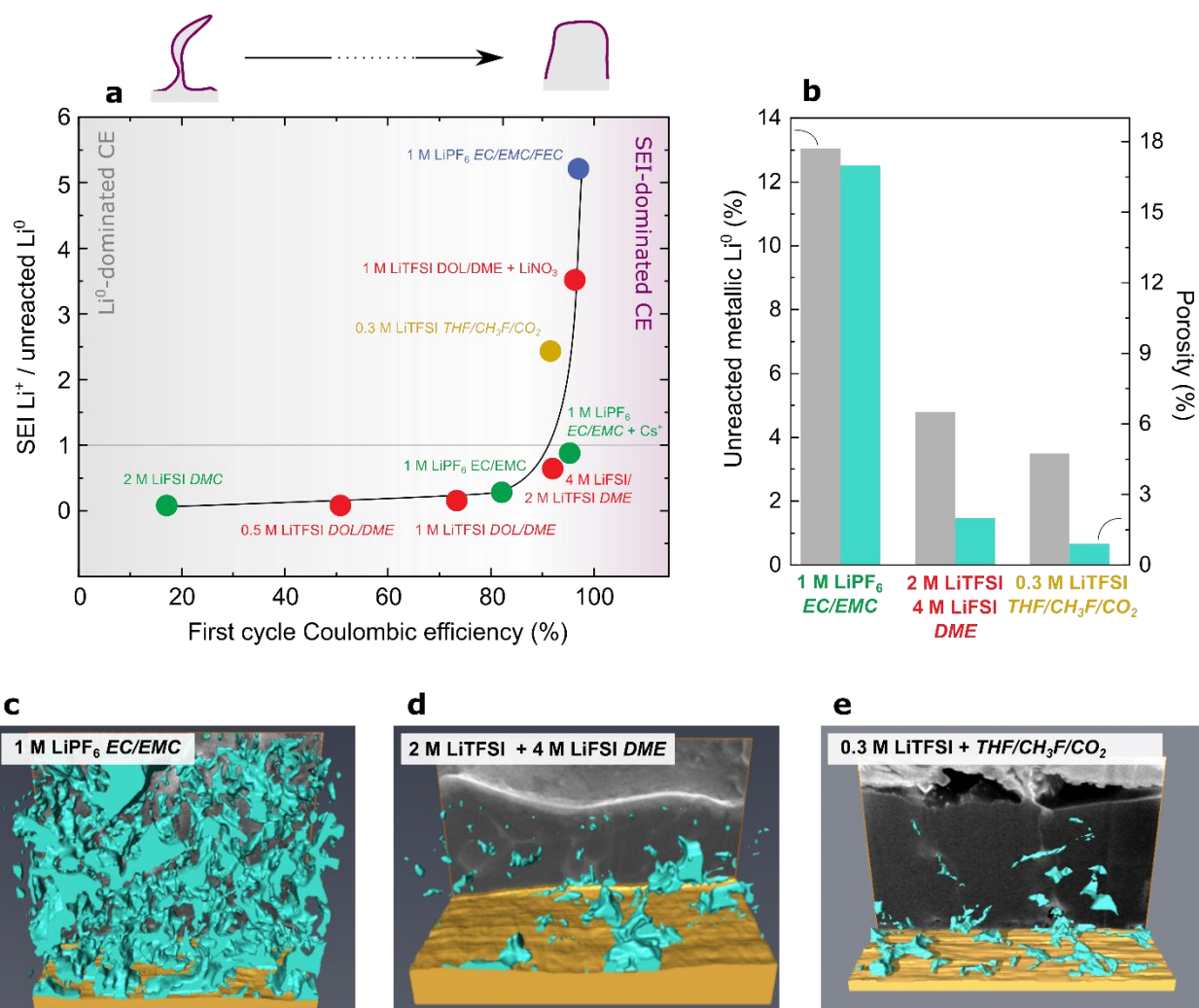


Figure 3 | Quantifying morphology and composition of electrochemically-inactive Li. (a) Ratio of capacity lost as SEI Li⁺ to capacity lost as encapsulated unreacted Li⁰ as a function of first cycle CE for various electrolytes. The latter was quantified by titration gas chromatography (TGC).^{35,39} The solid line serves as a visual guide but does not correspond to a fit. (b) Irreversible Li⁰ quantified by TGC (gray bars) and porosity quantified by focused ion beam (FIB) milling followed by computational 3D reconstruction from cryogenic transmission electron microscopy imaging (teal bars) for three representative electrolytes.⁴⁰ (c-e) Computational reconstruction of voids/pores after a plating half-cycle (1 mAh/cm²) for three representative electrolytes.⁴⁰ Teal represents voids. (b-e) were adapted from Lee *et al*⁴⁰ with permission from ACS Publications.

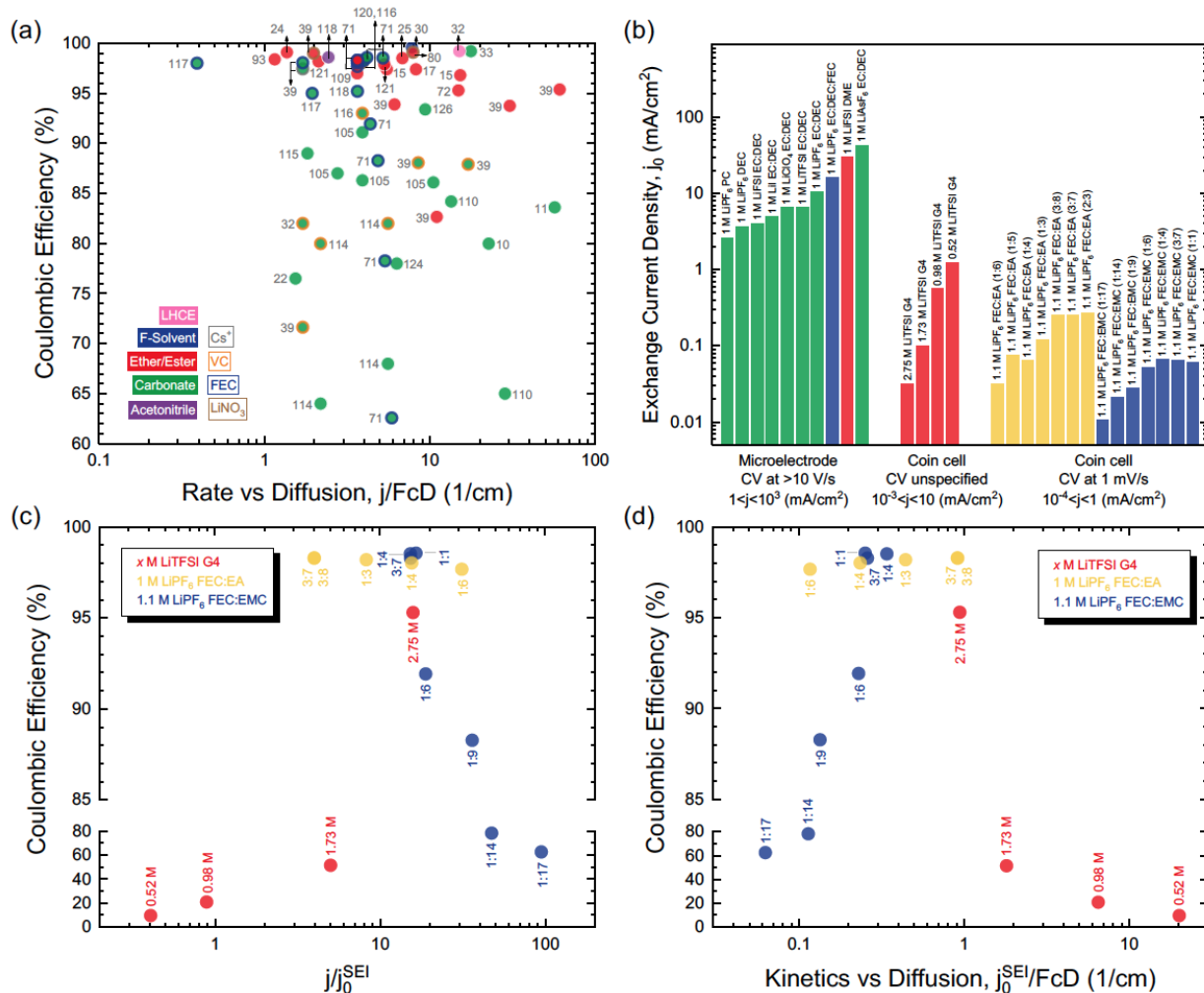


Figure 4 | Interplay between Li⁺ transport and redox kinetics. (a) Influence of electrolyte Li⁺ diffusivity and applied current density on Li plating and stripping CE. A detailed description of the electrolytes, their relative properties and CE is reported in the **Source Data**. (b) Exchange current density in various electrolytes, organized by measurement protocol.^{50,71,72} (c) Influence of the electrolyte-dependent exchange current density j_0 on CE measured in the presence of an SEI (low scan rate, 1 mV/s).^{71,72} (d) Correlation between exchange current density, Li⁺ diffusivity and CE.^{71,72} Calculations for Li⁺ diffusivity values are shown in the **Source Data** file and references used are aggregated here.^{24,28,30,32,71,73,109,118,121,125-132}

References

- 1 Nitta, N., Wu, F., Lee, J. T. & Yushin, G. Li-ion battery materials: present and future. *Mater. Today* **18**, 252-264, (2015).
- 2 U.S. Drive Electrochemical Energy Storage Technical Team Roadmap. *Vehicles Technologies Office. US Department of Energy.* (2017). <https://www.energy.gov/sites/default/files/2017/11/f39/EESTT%20roadmap%202017-10-16%20Final.pdf>
- 3 Xiao, J. *et al.* Understanding and applying coulombic efficiency in lithium metal batteries. *Nat. Energy*, 1-8, (2020).
- 4 Gauthier, M. *et al.* Electrode–Electrolyte Interface in Li-Ion Batteries: Current Understanding and New Insights. *J. Phys. Chem. Lett.* **6**, 4653-4672, (2015).
- 5 Peled, E. The Electrochemical Behavior of Alkali and Alkaline Earth Metals in Nonaqueous Battery Systems—The Solid Electrolyte Interphase Model. *Journal of the Electrochemical Society* **126**, 2047-2051, (1979).
- 6 Xu, K. Nonaqueous Liquid Electrolytes for Lithium-Based Rechargeable Batteries. *Chem. Rev.* **104**, 4303-4418, (2004).
- 7 Goodenough, J. B. & Kim, Y. Challenges for Rechargeable Li Batteries. *Chemistry of Materials* **22**, 587-603, (2010).
- 8 Fong, R., von Sacken, U. & Dahn, J. R. Studies of Lithium Intercalation into Carbons Using Nonaqueous Electrochemical Cells. *Journal of the Electrochemical Society* **137**, 2009-2013, (1990).
- 9 Harris, W. S. *Electrochemical studies in cyclic esters*, (1958).
- 10 Selim, R. & Bro, P. Some Observations on Rechargeable Lithium Electrodes in a Propylene Carbonate Electrolyte. *Journal of The Electrochemical Society* **121**, 1457-1457, (1974).
- 11 Rauh, R. D. & Brummer, S. B. The effect of additives on lithium cycling in propylene carbonate. *Electrochim. Acta* **22**, 75-83, (1977).
- 12 Heiskanen, S. K., Kim, J. & Lucht, B. L. Generation and Evolution of the Solid Electrolyte Interphase of Lithium-Ion Batteries. *Joule*, (2019).
- 13 Koch, V. R. & Young, J. H. The Stability of the Secondary Lithium Electrode in Tetrahydrofuran-Based Electrolytes. *Journal of the Electrochemical Society* **125**, 1371-1377, (1978).
- 14 Koch, V. R. Reactions of Tetrahydrofuran and Lithium Hexafluoroarsenate with Lithium. *Journal of the Electrochemical Society* **126**, 181-187, (1979).
- 15 Goldman, J. L., Mank, R. M., Young, J. H. & Koch, V. R. Structure-Reactivity Relationships of Methylated Tetrahydrofurans with Lithium. *Journal of The Electrochemical Society* **127**, 1461-1467, (1980).
- 16 Koch, V. R. Specular Lithium Deposits from Lithium Hexafluoroarsenate/Diethyl Ether Electrolytes. *Journal of the Electrochemical Society* **129**, 1-1, (1982).
- 17 Koch, V. R. & Young, J. H. 2-Methyltetrahydrofuran-Lithium Hexafluoroarsenate: A Superior Electrolyte for the Secondary Lithium Electrode. *Science* **204**, 499-501, (1979).
- 18 Foos, J. S. & Stolki, T. J. A New Ether Solvent for Lithium Cells. *Journal of the Electrochemical Society* **135**, 2769-2771, (1988).
- 19 Malik, Y., Aurbach, D., Dan, P. & Meitav, A. The electrochemical behaviour of 2-methyltetrahydrofuran solutions. *J. Electroanal. Chem.* **282**, 73-105, (1990).

- 20 Gofer, Y., Ben-Zion, M. & Aurbach, D. Solutions of LiAsF₆ in 1,3-dioxolane for secondary lithium batteries. *Journal of Power Sources* **39**, 163-178, (1992).
- 21 Wang, C., Meng, Y. S. & Xu, K. Perspective—Fluorinating Interphases. *Journal of The Electrochemical Society* **166**, A5184-A5186, (2018).
- 22 Ding, F. *et al.* Effects of Carbonate Solvents and Lithium Salts on Morphology and Coulombic Efficiency of Lithium Electrode. *Journal of The Electrochemical Society* **160**, A1894-A1901, (2013).
- 23 Miao, R. *et al.* Novel dual-salts electrolyte solution for dendrite-free lithium-metal based rechargeable batteries with high cycle reversibility. *Journal of Power Sources* **271**, 291-297, (2014).
- 24 Qian, J. *et al.* High rate and stable cycling of lithium metal anode. *Nat. Comm.* **6**, 1-9, (2015).
- 25 Suo, L., Hu, Y.-S., Li, H., Armand, M. & Chen, L. A new class of Solvent-in-Salt electrolyte for high-energy rechargeable metallic lithium batteries. *Nat. Comm.* **4**, 1481, (2013).
- 26 Fan, X. *et al.* Highly Fluorinated Interphases Enable High-Voltage Li-Metal Batteries. *Chem* **4**, 174-185, (2018).
- 27 Zeng, Z. *et al.* Non-flammable electrolytes with high salt-to-solvent ratios for Li-ion and Li-metal batteries. *Nat. Energy* **3**, 674-681, (2018).
- 28 Wang, J. *et al.* Superconcentrated electrolytes for a high-voltage lithium-ion battery. *Nat. Comm.* **7**, 12032, (2016).
- 29 Perez Beltran, S., Cao, X., Zhang, J.-G. & Balbuena, P. B. Localized High Concentration Electrolytes for High Voltage Lithium–Metal Batteries: Correlation between the Electrolyte Composition and Its Reductive/Oxidative Stability. *Chemistry of Materials* **32**, 5973-5984, (2020).
- 30 Suo, L. *et al.* Fluorine-donating electrolytes enable highly reversible 5-V-class Li metal batteries. *Proc. Natl. Acad. Sci. U.S.A.* **115**, 1156-1161, (2018).
- 31 Qiu, F. *et al.* A Concentrated Ternary-Salts Electrolyte for High Reversible Li Metal Battery with Slight Excess Li. *Adv. Energy Mater.* **9**, 1803372-1803372, (2019).
- 32 Chen, S. *et al.* High-Efficiency Lithium Metal Batteries with Fire-Retardant Electrolytes. *Joule* **2**, 1548-1558, (2018).
- 33 Chen, S. *et al.* High-Voltage Lithium-Metal Batteries Enabled by Localized High-Concentration Electrolytes. *Adv. Mater.* **30**, (2018).
- 34 Rustomji, C. S. *et al.* Liquefied gas electrolytes for electrochemical energy storage devices. *Science* **356**, eaal4263, (2017).
- 35 Yang, Y. *et al.* High-Efficiency Lithium-Metal Anode Enabled by Liquefied Gas Electrolytes. *Joule* **3**, 1986-2000, (2019).
- 36 Yang, Y. *et al.* Liquefied gas electrolytes for wide-temperature lithium metal batteries. *Energy Environ. Sci.* **13**, 2209-2219, (2020).
- 37 Fan, X. *et al.* Non-flammable electrolyte enables Li-metal batteries with aggressive cathode chemistries. *Nat. Nanotech.* **13**, 1-8, (2018).
- 38 Peled, E., Golodnitsky, D. & Ardel, G. Advanced Model for Solid Electrolyte Interphase Electrodes in Liquid and Polymer Electrolytes. *Journal of The Electrochemical Society* **144**, L208-L210, (1997).
- 39 Fang, C. *et al.* Quantifying inactive lithium in lithium metal batteries. *Nature* **572**, 511-515, (2019).

- 40 Lee, J. Z. *et al.* Cryogenic Focused Ion Beam Characterization of Lithium Metal Anodes. *ACS Energy Lett.* **4**, 489-493, (2019).
- 41 Nagpure, S. C. *et al.* Impacts of lean electrolyte on cycle life for rechargeable Li metal batteries. *Journal of Power Sources* **407**, 53-62, (2018).
- 42 Lu, D. *et al.* Failure Mechanism for Fast-Charged Lithium Metal Batteries with Liquid Electrolytes. *Adv. Energy Mater.* **5**, 1400993, (2015).
- 43 Louli, A. J., Ellis, L. D. & Dahn, J. R. Operando Pressure Measurements Reveal Solid Electrolyte Interphase Growth to Rank Li-Ion Cell Performance. *Joule*, (2019).
- 44 Louli, A. J. *et al.* Diagnosing and correcting anode-free cell failure via electrolyte and morphological analysis. *Nat. Energy* **5**, 693-702, (2020).
- 45 Hsieh, Y.-C. *et al.* Quantification of Dead Lithium via In Situ Nuclear Magnetic Resonance Spectroscopy. *Cell Rep. Phys. Sci.* **1**, 100139, (2020).
- 46 Gunnarsdóttir, A. B., Amanchukwu, C. V., Menkin, S. & Grey, C. P. Noninvasive In Situ NMR Study of “Dead Lithium” Formation and Lithium Corrosion in Full-Cell Lithium Metal Batteries. *Journal of the American Chemical Society* **142**, 20814-20827, (2020).
- 47 Popov, K. I., Djokić, S. S., Nikolić, N. D. & Jović, V. D. *Morphology of electrochemically and chemically deposited metals.* (Springer, 2016).
- 48 Barton, J. L., Bockris, J. O., apos, m & Ubbelohde, A. R. J. P. The electrolytic growth of dendrites from ionic solutions. *Proceedings of the Royal Society of London. Series A. Mathematical and Physical Sciences* **268**, 485-505, (1962).
- 49 Cohen, Y. S., Cohen, Y. & Aurbach, D. Micromorphological Studies of Lithium Electrodes in Alkyl Carbonate Solutions Using in Situ Atomic Force Microscopy. *The Journal of Physical Chemistry B* **104**, 12282-12291, (2000).
- 50 Boyle, D. T. *et al.* Transient Voltammetry with Ultramicroelectrodes Reveals the Electron Transfer Kinetics of Lithium Metal Anodes. *ACS Energy Lett.* **5**, 701-709, (2020).
- 51 Liu, S. *et al.* Lithium Dendrite Formation in Li/Poly(ethylene oxide)–Lithium Bis(trifluoromethanesulfonyl)imide and N-Methyl-N-propylpiperidinium Bis(trifluoromethanesulfonyl)imide/Li Cells. *Journal of the Electrochemical Society* **157**, A1092, (2010).
- 52 Gireaud, L., Grugeon, S., Laruelle, S., Yrieix, B. & Tarascon, J. M. Lithium metal stripping/plating mechanisms studies: A metallurgical approach. *Electrochem. Commun.* **8**, 1639-1649, (2006).
- 53 Rosso, M., Gobron, T., Brissot, C., Chazalviel, J. N. & Lascaud, S. Onset of dendritic growth in lithium/polymer cells. *Journal of Power Sources* **97-98**, 804-806, (2001).
- 54 Sand, H. J. S. III. On the concentration at the electrodes in a solution, with special reference to the liberation of hydrogen by electrolysis of a mixture of copper sulphate and sulphuric acid. *Philos. Mag.* **1**, 45-79, (1901).
- 55 Mayers, M. Z., Kaminski, J. W. & Miller, T. F. Suppression of Dendrite Formation via Pulse Charging in Rechargeable Lithium Metal Batteries. *J. Phys. Chem. C* **116**, 26214-26221, (2012).
- 56 Monroe, C. & Newman, J. The Impact of Elastic Deformation on Deposition Kinetics at Lithium/Polymer Interfaces. *Journal of the Electrochemical Society* **152**, A396, (2005).
- 57 Tikekar, M. D., Choudhury, S., Tu, Z. & Archer, L. A. Design principles for electrolytes and interfaces for stable lithium-metal batteries. *Nat. Energy* **1**, 16114, (2016).
- 58 Maslyn, J. A. *et al.* Preferential Stripping of a Lithium Protrusion Resulting in Recovery of a Planar Electrode. *Journal of the Electrochemical Society* **167**, 100553, (2020).

- 59 Arakawa, M., Tobishima, S.-i., Nemoto, Y., Ichimura, M. & Yamaki, J.-i. Lithium electrode cycleability and morphology dependence on current density. *Journal of Power Sources* **43**, 27-35, (1993).
- 60 Liang, Z. *et al.* Composite lithium metal anode by melt infusion of lithium into a 3D conducting scaffold with lithiophilic coating. *Proc. Natl. Acad. Sci. U.S.A.* **113**, 2862, (2016).
- 61 Lin, D. *et al.* Layered reduced graphene oxide with nanoscale interlayer gaps as a stable host for lithium metal anodes. *Nat. Nanotech.* **11**, 626-632, (2016).
- 62 Liu, Y. *et al.* Lithium-coated polymeric matrix as a minimum volume-change and dendrite-free lithium metal anode. *Nat. Comm.* **7**, 10992, (2016).
- 63 Louli, A. J. *et al.* Exploring the Impact of Mechanical Pressure on the Performance of Anode-Free Lithium Metal Cells. *Journal of The Electrochemical Society* **166**, A1291-A1299, (2019).
- 64 Fang, C. *et al.* Pressure-tailored lithium deposition and dissolution in lithium metal batteries. *arXiv preprint arXiv:2008.07710*, (2020).
- 65 Lopez, J. *et al.* Effects of Polymer Coatings on Electrodeposited Lithium Metal. *Journal of the American Chemical Society* **140**, 11735-11744, (2018).
- 66 Yu, Z. *et al.* A Dynamic, Electrolyte-Blocking, and Single-Ion-Conductive Network for Stable Lithium-Metal Anodes. *Joule* **3**, 2761-2776, (2019).
- 67 Stalin, S. *et al.* Designing Polymeric Interphases for Stable Lithium Metal Deposition. *Nano Lett.* **20**, 5749-5758, (2020).
- 68 Guo, R. & Gallant, B. M. Li₂O Solid Electrolyte Interphase: Probing Transport Properties at the Chemical Potential of Lithium. *Chemistry of Materials* **32**, 5525-5533, (2020).
- 69 Benitez, L. & Seminario, J. M. Ion Diffusivity through the Solid Electrolyte Interphase in Lithium-Ion Batteries. *Journal of the Electrochemical Society* **164**, E3159-E3170, (2017).
- 70 Lowe, J. S. & Siegel, D. J. Modeling the Interface between Lithium Metal and Its Native Oxide. *ACS Appl. Mater. Interfaces* **12**, 46015-46026, (2020).
- 71 Su, C.-C. *et al.* Solvation Rule for Solid-Electrolyte Interphase Enabler in Lithium-Metal Batteries. *Angew. Chem. Int. Ed.* **59**, 18229-18233, (2020).
- 72 Liu, Y. *et al.* Insight into the Critical Role of Exchange Current Density on Electrodeposition Behavior of Lithium Metal. *Adv. Sci.* **n/a**, 2003301, (2021).
- 73 Tao, R. *et al.* Kinetics Tuning the Electrochemistry of Lithium Dendrites Formation in Lithium Batteries through Electrolytes. *ACS Appl. Mater. Interfaces* **9**, 7003-7008, (2017).
- 74 Shi, F. *et al.* Strong texturing of lithium metal in batteries. *Proc. Natl. Acad. Sci. U.S.A.* **114**, 12138, (2017).
- 75 He, M., Guo, R., Hobold, G. M., Gao, H. & Gallant, B. M. The intrinsic behavior of lithium fluoride in solid electrolyte interphases on lithium. *Proc. Natl. Acad. Sci. U.S.A.* **117**, 73-79, (2020).
- 76 Zhang, Q. *et al.* Synergetic Effects of Inorganic Components in Solid Electrolyte Interphase on High Cycle Efficiency of Lithium Ion Batteries. *Nano Lett.* **16**, 2011-2016, (2016).
- 77 Aurbach, D., Ein-Ely, Y. & Zaban, A. The surface chemistry of lithium electrodes in alkyl carbonate solutions. *Journal of the Electrochemical Society* **141**, (1994).
- 78 Xue, W. *et al.* Ultra-high-voltage Ni-rich layered cathodes in practical Li metal batteries enabled by a sulfonamide-based electrolyte. *Nat. Energy*, (2021).

- 79 Xue, W. *et al.* FSI-inspired solvent and “full fluorosulfonyl” electrolyte for 4 V class lithium-metal batteries. *Energy Environ. Sci.* **13**, 212-220, (2020).
- 80 Li, W. *et al.* The synergetic effect of lithium polysulfide and lithium nitrate to prevent lithium dendrite growth. *Nature Communications* **6**, 1-8, (2015).
- 81 Zhu, Y. *et al.* Design principles for self-forming interfaces enabling stable lithium-metal anodes. *Proc. Natl. Acad. Sci. U.S.A.* **117**, 27195, (2020).
- 82 Li, Y. *et al.* Correlating Structure and Function of Battery Interphases at Atomic Resolution Using Cryoelectron Microscopy. *Joule* **2**, 2167-2177, (2018).
- 83 Li, Y. *et al.* Atomic structure of sensitive battery materials and interfaces revealed by cryo-electron microscopy. *Science* **358**, 506, (2017).
- 84 Zachman, M. J., Tu, Z., Choudhury, S., Archer, L. A. & Kourkoutis, L. F. Cryo-STEM mapping of solid-liquid interfaces and dendrites in lithium-metal batteries. *Nature* **560**, 345-349, (2018).
- 85 Huang, W., Wang, H., Boyle, D. T., Li, Y. & Cui, Y. Resolving Nanoscopic and Mesoscopic Heterogeneity of Fluorinated Species in Battery Solid-Electrolyte Interphases by Cryogenic Electron Microscopy. *ACS Energy Lett.* **5**, 1128-1135, (2020).
- 86 Michan, A. L. *et al.* Fluoroethylene Carbonate and Vinylene Carbonate Reduction: Understanding Lithium-Ion Battery Electrolyte Additives and Solid Electrolyte Interphase Formation. *Chemistry of Materials* **28**, 8149-8159, (2016).
- 87 Hobold, G. M., Khurram, A. & Gallant, B. M. Operando Gas Monitoring of Solid Electrolyte Interphase Reactions on Lithium. *Chemistry of Materials*, (2020).
- 88 Zhang, Y. *et al.* Revealing electrolyte oxidation via carbonate dehydrogenation on Ni-based oxides in Li-ion batteries by in situ Fourier transform infrared spectroscopy. *Energy Environ. Sci.* **13**, 183-199, (2020).
- 89 Wang, H. *et al.* Efficient Lithium Metal Cycling over a Wide Range of Pressures from an Anion-Derived Solid-Electrolyte Interphase Framework. *ACS Energy Lett.* **6**, 816-825, (2021).
- 90 Niu, C. *et al.* Balancing interfacial reactions to achieve long cycle life in high-energy lithium metal batteries. *Nat. Energy*, (2021).
- 91 Yang, H., Kwon, K., Devine, T. M. & Evans, J. W. Aluminum Corrosion in Lithium Batteries An Investigation Using the Electrochemical Quartz Crystal Microbalance. *Journal of The Electrochemical Society* **147**, 4399, (2000).
- 92 Kim, K. *et al.* Understanding the thermal instability of fluoroethylene carbonate in LiPF₆-based electrolytes for lithium ion batteries. *Electrochim. Acta* **225**, 358-368, (2017).
- 93 Yu, Z. *et al.* Molecular design for electrolyte solvents enabling energy-dense and long-cycling lithium metal batteries. *Nat. Energy* **5**, 526-533, (2020).
- 94 Alvarado, J. *et al.* A carbonate-free, sulfone-based electrolyte for high-voltage Li-ion batteries. *Mater. Today* **21**, 341-353, (2018).
- 95 Ren, X. *et al.* Localized High-Concentration Sulfone Electrolytes for High-Efficiency Lithium-Metal Batteries. *Chem* **4**, 1877-1892, (2018).
- 96 Li, W., Erickson, E. M. & Manthiram, A. High-nickel layered oxide cathodes for lithium-based automotive batteries. *Nat. Energy* **5**, 26-34, (2020).
- 97 Gao, H. & Gallant, B. M. Advances in the chemistry and applications of alkali-metal-gas batteries. *Nature Reviews Chemistry* **4**, 566-583, (2020).
- 98 Manthiram, A., Fu, Y., Chung, S.-H., Zu, C. & Su, Y.-S. Rechargeable Lithium-Sulfur Batteries. *Chem. Rev.* **114**, 11751-11787, (2014).

- 99 Zhang, Y. & Viswanathan, V. Design Rules for Selecting Fluorinated Linear Organic Solvents for Li Metal Batteries. *J. Phys. Chem. Lett.*, 5821-5828, (2021).
- 100 Adams, B. D., Zheng, J., Ren, X., Xu, W. & Zhang, J. G. Accurate Determination of Coulombic Efficiency for Lithium Metal Anodes and Lithium Metal Batteries. *Adv. Energy Mater.* **8**, (2018).
- 101 Bond, T. M., Burns, J. C., Stevens, D. A., Dahn, H. M. & Dahn, J. R. Improving Precision and Accuracy in Coulombic Efficiency Measurements of Li-Ion Batteries. *Journal of The Electrochemical Society* **160**, A521-A527, (2013).
- 102 Ye, H. *et al.* Synergism of Al-containing solid electrolyte interphase layer and Al-based colloidal particles for stable lithium anode. *Nano Energy* **36**, 411-417, (2017).
- 103 Zheng, J. *et al.* Manipulating electrolyte and solid electrolyte interphase to enable safe and efficient Li-S batteries. *Nano Energy* **50**, 431-440, (2018).
- 104 Cao, X. *et al.* Monolithic solid–electrolyte interphases formed in fluorinated orthoformate-based electrolytes minimize Li depletion and pulverization. *Nat. Energy* **4**, 796-805, (2019).
- 105 Genovese, M. *et al.* Combinatorial Methods for Improving Lithium Metal Cycling Efficiency. *Journal of The Electrochemical Society* **165**, A3000-A3013, (2018).
- 106 Aurbach, D., Youngman, O., Gofer, Y. & Meitav, A. The electrochemical behaviour of 1,3-dioxolane—LiClO₄ solutions—I. Uncontaminated solutions. *Electrochim. Acta* **35**, 625-638, (1990).
- 107 Jurng, S., Brown, Z. L., Kim, J. & Lucht, B. L. Effect of electrolyte on the nanostructure of the solid electrolyte interphase (SEI) and performance of lithium metal anodes. *Energy Environ. Sci.* **11**, 2600-2608, (2018).
- 108 Schedlbauer, T. *et al.* Lithium difluoro(oxalato)borate: A promising salt for lithium metal based secondary batteries? *Electrochim. Acta* **92**, 102-107, (2013).
- 109 Fang, Z. *et al.* Novel Concentrated Li[(FSO₂)(n-C₄F₉SO₂)N]-Based Ether Electrolyte for Superior Stability of Metallic Lithium Anode. **9**, 4282-4289, (2017).
- 110 Rauh, R. D., Reise, T. F. & Brummer, S. B. Efficiencies of Cycling Lithium on a Lithium Substrate in Propylene Carbonate. *Journal of The Electrochemical Society* **125**, 186-190, (1978).
- 111 Aurbach, D. The Correlation Between Surface Chemistry, Surface Morphology, and Cycling Efficiency of Lithium Electrodes in a Few Polar Aprotic Systems. *Journal of The Electrochemical Society* **136**, 3198-3198, (1989).
- 112 Aurbach, D. & Gofer, Y. The Behavior of Lithium Electrodes in Mixtures of Alkyl Carbonates and Ethers. *Journal of The Electrochemical Society* **138**, 3529-3536, (1991).
- 113 Foos, J. S. & McVeigh, J. Lithium Cycling in Polymethoxymethane Solvents. *Journal of The Electrochemical Society* **130**, 628-630, (1983).
- 114 Ota, H., Shima, K., Ue, M. & Yamaki, J.-i. Effect of vinylene carbonate as additive to electrolyte for lithium metal anode. *Electrochim. Acta* **49**, 565-572, (2004).
- 115 Markevich, E., Salitra, G., Chesneau, F., Schmidt, M. & Aurbach, D. Very Stable Lithium Metal Stripping-Plating at a High Rate and High Areal Capacity in Fluoroethylene Carbonate-Based Organic Electrolyte Solution. *ACS Energy Lett.* **2**, 1321-1326, (2017).
- 116 Liu, Y. *et al.* Solubility-mediated sustained release enabling nitrate additive in carbonate electrolytes for stable lithium metal anode. *Nat. Comm.* **9**, 3656, (2018).

- 117 Zhang, X.-Q., Cheng, X.-B., Chen, X., Yan, C. & Zhang, Q. Fluoroethylene Carbonate Additives to Render Uniform Li Deposits in Lithium Metal Batteries. *Adv. Funct. Mater.* **27**, 1605989, (2017).
- 118 Peng, Z. *et al.* High-Power Lithium Metal Batteries Enabled by High-Concentration Acetonitrile-Based Electrolytes with Vinylene Carbonate Additive. *Adv. Funct. Mater.*, 2001285-2001285, (2020).
- 119 Brown, Z. L., Jurng, S. & Lucht, B. L. Investigation of the Lithium Solid Electrolyte Interphase in Vinylene Carbonate Electrolytes Using Cu||LiFePO₄ Cells. *Journal of The Electrochemical Society* **164**, A2186-A2189, (2017).
- 120 Brown, Z. L., Jurng, S., Nguyen, C. C. & Lucht, B. L. Effect of Fluoroethylene Carbonate Electrolytes on the Nanostructure of the Solid Electrolyte Interphase and Performance of Lithium Metal Anodes. *ACS Applied Energy Materials* **1**, 3057-3062, (2018).
- 121 Alvarado, J. *et al.* Bisalt ether electrolytes: A pathway towards lithium metal batteries with Ni-rich cathodes. *Energy and Environmental Science* **12**, 780-794, (2019).
- 122 Amanchukwu, C. V. *et al.* A New Class of Ionically Conducting Fluorinated Ether Electrolytes with High Electrochemical Stability. *Journal of the American Chemical Society* **142**, 7393-7403, (2020).
- 123 Holoubek, J. *et al.* An All-Fluorinated Ester Electrolyte for Stable High-Voltage Li Metal Batteries Capable of Ultra-Low-Temperature Operation. *ACS Energy Lett.* **5**, 1438-1447, (2020).
- 124 Aurbach, D., Markovsky, B., Shechter, A., Ein-Eli, Y. & Cohen, H. A comparative study of synthetic graphite and Li electrodes in electrolyte solutions based on ethylene carbonate-dimethyl carbonate mixtures. *Journal of The Electrochemical Society* **143**, 3809-3820, (1996).
- 125 Tomas Gottwald & Vondrak, J. in *Proceedings of the 23rd Conference STUDENT EEICT 2017*. 522-526.
- 126 Nilsson, V., Kotronia, A., Lacey, M., Edström, K. & Johansson, P. Highly Concentrated LiTFSI-EC Electrolytes for Lithium Metal Batteries. *ACS Applied Energy Materials* **3**, 200-207, (2020).
- 127 Dahbi, M., Ghamouss, F., Tran-Van, F., Lemordant, D. & Anouti, M. Comparative study of EC/DMC LiTFSI and LiPF₆ electrolytes for electrochemical storage. *Journal of Power Sources* **196**, 9743-9750, (2011).
- 128 Xia, L. *et al.* Fluorinated Electrolytes for Li-Ion Batteries: The Lithium Difluoro(oxalato)borate Additive for Stabilizing the Solid Electrolyte Interphase. *ACS Omega* **2**, 8741-8750, (2017).
- 129 Frenck, L., Sethi, G. K., Maslyn, J. A. & Balsara, N. P. Factors That Control the Formation of Dendrites and Other Morphologies on Lithium Metal Anodes. *Frontiers in Energy Research* **7**, (2019).
- 130 Beyene, T. T. *et al.* Concentrated Dual-Salt Electrolyte to Stabilize Li Metal and Increase Cycle Life of Anode Free Li-Metal Batteries. *Journal of The Electrochemical Society* **166**, A1501-A1509, (2019).
- 131 Abouimrane, A., Ding, J. & Davidson, I. J. Liquid electrolyte based on lithium bis-fluorosulfonyl imide salt: Aluminum corrosion studies and lithium ion battery investigations. *Journal of Power Sources* **189**, 693-696, (2009).

- 132 Zhang, C. *et al.* Chelate Effects in Glyme/Lithium Bis(trifluoromethanesulfonyl)amide Solvate Ionic Liquids. I. Stability of Solvate Cations and Correlation with Electrolyte Properties. *J. Phys. Chem. B* **118**, 5144-5153, (2014).